

# Unsupervised Object Localization using Generative Adversarial Networks

Junsuk Choe, Joo Hyun Park, Hyunjung Shim

Yonsei University

**Abstract.** This paper introduces a novel end-to-end deep neural network model for unsupervised object localization for the first time. We adopt Generative Adversarial Networks (GANs) to object localization framework, where GANs are powerful tools that implicitly learn the unknown data distribution in an unsupervised manner. It is because we observe that GAN discriminator is highly influenced by pixels where objects appear. Motivated by this observation, we apply an existing technique that visualizes important pixels for classification to the discriminator. Based on extensive evaluations and experimental studies, the proposed approach achieves meaningful accuracy for unsupervised object localization using public benchmark datasets, even comparable to state-of-the-art weakly-supervised approach.

**Keywords:** Object Localization; Unsupervised Machine Learning; End-to-end Deep Learning; Generative Adversarial Networks; Mode Collapse

## 1 Introduction

Object localization aims to identify the location of a target object in a given scene. Recently, deep learning based methods such as Faster R-CNN [1], YOLO [2], SSD [3] have achieved significant improvement in object detection with real-time performance. These techniques [1,2,3,4,5,6,7,8,9,10,11], however, utilize fully-supervised learning, that require category labels and bounding box annotations for training. Because such information is considered expensive, acquiring massive amount of data is difficult, drawing a limit for practical applications.

To alleviate the burden on data annotation, weakly-supervised learning methods have been suggested. Weakly-supervised object localization uses only category labels during training, thus the data annotation becomes manageable. Among those, Class Activation Mapping (CAM) [12] is a representative weakly-supervised object localization method. CAM is designed to extract a heatmap by visualizing internal layer of CNN, and post-process to find a bounding box. The main idea of CAM is that the pixels contributing to object classification coincide with the object location. However, even the cheapest information, object categories, may not be affordable in many applications.

For a fundamental solution to annotation dependency, unsupervised object localization techniques have emerged. This problem is considered even more challenging than fully-supervised, or weakly-supervised object localization, in a

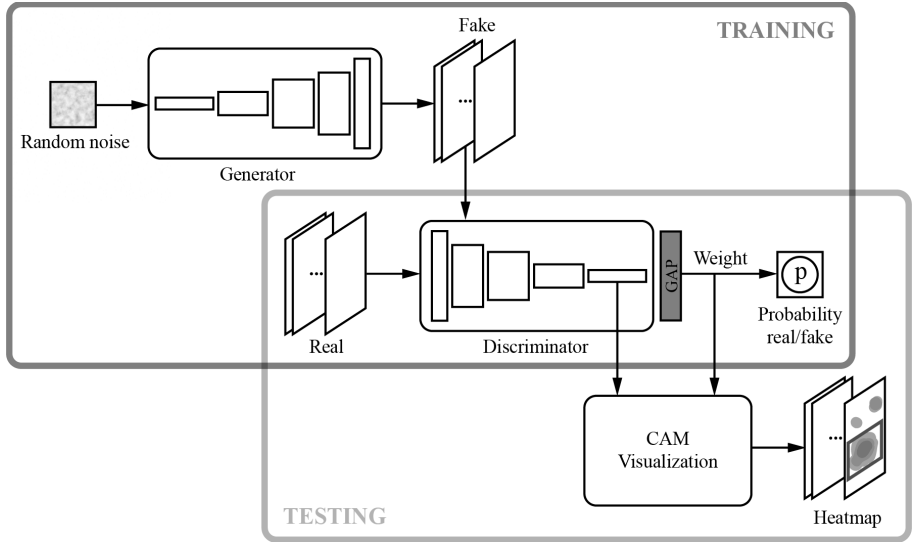


**Fig. 1.** Block diagram of the proposed method. The GAN model is trained in a fully-unsupervised scheme. GAP denotes Global Average Pooling (GAP) layer. In testing phase, the heatmap is extracted from the internal layer of a GAN discriminator using CAM.

sense that there is no additional information other than the given images. Unlike supervised, or weakly-supervised methods, unsupervised object localization techniques are yet to employ deep neural networks. Traditional techniques such as [13,14,15,16,17] still rely on hand-crafted feature extractions, graph-based theories, or optimization, placing a limit to real-time performance. Meanwhile, deep neural network models are considered outstanding in feature extraction, outperforming previous hand-crafted ones in most pattern recognition problems, even achieving real-time performance. Motivated by their recent success, we aim to apply deep neural networks to unsupervised object localization, expecting improvements in both performance and time efficiency. More specifically, in this paper, we suggest an end-to-end unsupervised object localization method based on Generative Adversarial Networks (GANs) [18] for the first time.

GAN is an unsupervised generative model, that learns to generate the true data distribution by implicit density estimation. GAN is composed of a generator and a discriminator. In training, the generator is trained in a way the discriminator cannot distinguish fake images produced by the generator. Meanwhile, the discriminator learns to distinguish them from real images. Through this adversarial competition, the generated images from GAN become harder to distinguish from the reals. Among many generative models, GAN is known to generate most sharp and realistic images.

In this paper, we take advantage of a GAN discriminator for unsupervised object localization. Without utilizing priors or annotations, GAN successfully

generates images that follow the data distributions. If the generator is trained to produce a dominant object (i.e., the most frequently appearing object), we expect that the discriminator will pay more attention to the spatial location of the dominant object in distinguishing real or fake.

However, a GAN discriminator may not always use the dominant object as a decision criteria. Natural images can include various objects other than the dominant object. If the GAN model also learns those of various objects, this means that the discriminator exam not only the dominant object, but also other objects or background for discriminating real and fake.

Interestingly, generating various objects is directly associated with the diverse image generation in GAN training. Recent advance of GAN training tends to modify the loss function [19], or adds a regularization term [20,21] to encourage diverse image generations. Meanwhile, early models of GAN are limited to learn only the major modes of data distribution. The consequent phenomenon is called *mode collapse*, major issue in GAN training.

Although this mode collapse is considered undesirable, we expect this pathological behavior is rather useful in our application; We observed that the most frequently appearing object in the dataset is generated when mode collapse occurs. Based on this observation, we regard that a dominant object corresponds to a major mode in a data distribution. For this reason, we choose an early GAN model for our object localization.

The proposed method trains a GAN model in an unsupervised manner, and extracts a heatmap from the trained discriminator using CAM. Then, the heatmap is post-processed to determine the bounding box for object localization. Fig. 1 shows the block diagram of our approach. Within the whole process, neither supervision, nor any extra labeling information, such as negative sampling, is required.

Our model receives a single image as an input, and outputs a heatmap, or a bounding box. By leveraging publicly available datasets, we demonstrate the feasibility of GAN for addressing the problem of unsupervised object localization. Furthermore, we show that quantitative and qualitative performance of our model is plausible compared to the ones with weakly-supervised object localization. To our best knowledge, our proposition is the first end-to-end deep neural network model for unsupervised object localization, and we believe that this method can serve as an important baseline for the unsupervised object localization research.

## 2 Related works

In this section, we will review previous works of weakly-supervised and unsupervised approaches.

**Weakly-supervised object localization.** Weakly-supervised techniques utilize category labels, relatively low-cost annotations, to perform object localization. Traditional weakly-supervised approaches [22,23,24,25,26,27] mostly

learn patterns or features that best discriminate object categories from the others, and facilitate such information to localize objects. These methods, however, have a disadvantage that they only capture a fraction of an object, because localization is performed only with the most discriminative part of the object.

Unlike these conventional methods, recent weakly-supervised approaches utilize Deep Convolutional Neural Networks (CNNs) [12,28,29,30,31]. These approaches analyze the internal layer of CNN classifiers, pre-trained with category labels, for object localization. They extract a heatmap, also known as a saliency map, from the CNN classifier, then localize objects by processing it. However, similar to the traditional methods, these CNN-based approaches also cover only a fraction, not the whole object. In order to overcome such disadvantage, the latest techniques [32,33,34] have randomly removed the most discriminative parts from the image during training so that the network can consider the entire object.

**Unsupervised object localization.** Unsupervised approaches do not depend on additional annotations for object localization. This problem is very challenging in that there is no other information except for given images. For that, early techniques were designed under an assumption that only one object category exists in a dataset [13,14,15,16,35,36,37]. This method is known as co-localization, and is regarded as an unsupervised approach, since there are no additional supervisions during training. Recently, Wei et al. [36,37] proposed the usage of the deep features from a pre-trained CNN, and calculated their correlation for co-localization. Although this technique utilizes deep neural networks as a feature extractor, this is different from our method in that we develop an end-to-end network. Also, they only evaluate their performance with co-localization, not for fully-unsupervised settings.

Cho et al. [17] introduced a technique for performing object localization with a dataset containing multiple categories. Based on the off-the-shelf region proposal techniques, they used a Hough transform-based matching algorithm to assign scores to object candidates and performed object localization according to the scores. Meanwhile, Niu et. al [38] performed object localization using topic models [39]. They improved the localization performance by reformulating the existing Must-Link techniques [40] to overcome the *topic coherence* problem [41]. However, because these techniques rely on non-linear optimization, or graph modeling, the real-time performance is unlikely to be achieved. Unfortunately, the real-time performance is critical in many applications using object localization. Unlike previous methods, our method runs by the forward-propagation of deep neural networks, thus operate in real-time.

While the fully-supervised or weakly-supervised approaches actively adopt powerful deep neural networks, many unsupervised approaches still rely on hand-crafted features or optimization-based inference techniques. For unsupervised object localization, our approach adopts GAN [18], which is the most widely used model among unsupervised deep neural network models, and CAM [12], which is state-of-the-art technique for visualizing internal layers of CNN. We will explain the principle of GAN and CAM as a background of our proposed method in the next section.

### 3 Background

#### 3.1 Generative Adversarial Networks (GANs)

Recent approaches to improving GAN aims to achieve either the image quality or the image diversity (i.e., mode collapse). As mentioned in Section 1, mode collapse is closely related to the object localization. Hence, in this subsection, we will discuss the related work of GANs in respect of mode collapse.

Generative Adversarial Networks (GANs) was proposed by Goodfellow et al. [18] for the first time. Training of GAN can be done by adversarial competition between a generator and a discriminator. The discriminator outputs a probability of an input to be real. For training a generator, [18] suggested two different methods: a minimax GAN, and a non-saturating GAN. The minimax GAN derives that generated samples are unlikely to be fake. Meanwhile, the non-saturating GAN encourages that generated samples are more likely to be real.

Goodfellow et. al [18] used a minimax GAN to mathematically prove their method. However, they suggested that it is better to use a non-saturating GAN in practical applications due to gradient vanishing problem in the minimax GAN that occurs at the early stage of the training. To resolve, with large-scale study, Radford et. al [42] found optimal combination of network architectures and hyperparameters for the non-saturating GAN. This method is called Deep Convolutional GAN (DCGAN), the most widely used network architecture in developing GANs.

Arjovsky and Bottou [43] have shown that gradient vanishing or mode collapse arose because of the improper objective function. To address this problem, Arjovsky et. al [19] constructed a Wasserstein distance based objective function using Kantorovich-Rubinstein (KR) duality, which holds the weakest convergence property. To this end, they designed an objective function for the discriminator to meet the  $k$ -lipschitz condition by employing a weight clipping scheme.

To further improve WGAN, Gulrajani et. al [20] introduced a Gradient Penalty (GP) term for replacing the weight clipping used in WGAN. This method, commonly known as WGAN-GP, is regarded as one of state-of-the-art techniques for image generation. Meanwhile, recently, Kodali et. al [21] pointed out that GP term proposed by [20] violates the Kantorovich-Rubinstein (KR) duality; they proved that the KR duality is valid only if GAN reproduces the true data distribution sufficiently well. For the solution, they suggested a new GP term that based on the no-regret algorithm [44]. This method is called Deep Regret Analytic GAN (DRAGAN), and is also evaluated as a state-of-the-art technique with WGAN-GP. Later, Fedus et. al [45] replaced a minimax GAN with a non-saturating GAN for implementing DRAGAN (DRAGAN-NS), and showed experimentally that both GP terms improve the diverse image generation of the non-saturating GAN.

### 3.2 Class Activation Mapping (CAM)

CAM [12] visualizes the region where the CNN classifier, pre-trained with category labels, is influenced to decide a object category. For this, CAM replaces fully-connected layer of the CNN with Global Average Pooling (GAP) layer. In this way, we can conserve the spatial information of the image until the last layer.

The weight associating the last GAP layer and the classification layer indicates how important the each activation map of the last convolutional layer just before the GAP layer is. Exploiting this weight information, a heatmap of the target category can be extracted by the weighted sum of activation maps from the last convolutional layers. This heatmap is binarized by simple thresholding with pre-determined ratio of the maximum value. After that, they exam the connected components from binarized heatmap, draw the tightest bounding box for each connected component, and select the largest box.

## 4 Approaches

In this section, our approach to the proposed method will be explained in detail. We will first introduce proposed networks, and then explain the standards for selecting GANs and data augmentations. We will finally describe implementation details.

**Proposed networks.** We add a Global Average Pooling (GAP) layer at the end of the last convolutional layer of the GAN discriminator, and connect this GAP layer to the binary classification layer in a fully-connected manner. Note that the weight between the GAP layer and the classification layer of the previous CAM indicates how much the each activation map of the last convolution layer contributes to decide the category label. Likewise, our weight represents how much each activation map contributes in correctly distinguishing real and fake images. The extracted heatmap from such trained GAN can result in the bounding box by following the same post-processing applied for CAM. As shown in Fig. 1, we utilize both a generator and a discriminator in our training phase while we only use the discriminator in the test phase. In addition, we assume that there is only a single object in images like other weakly-supervised approaches [12,32,33,34]. This means the proposed approach will draw only one bounding box per image.

**Selected GANs.** Recent GAN models has made a meaningful progress toward preventing mode collapse, and attempts to encapsulate all modes of data distribution. This is equivalent to generating all objects appearing in the dataset. In such case, the discriminator is likely to consider the overall region of image for classification. It is because it learns not only the dominant object, but also other objects or the background, which appears relatively less. Although those GANs are superior to the early models of GAN in the perspective of generative power, they are disadvantageous for object localization.

On the other hand, early models of GAN easily fall into mode collapse, thus generate the dominant object, major mode, that frequently appears in the

dataset while ignoring objects that appears less in the dataset. One might argue that the major mode can correspond to not only major objects, but also textures or color characteristics. It is true that specific textures and colors are strongly correlated with major modes. However, most of them are strongly associated with dominant objects. Therefore, we believe that this is desirable for object localization and mode collapse can be positive for object localization.

We select three variants of GAN models: DCGAN, WGAN-GP, and DRAGAN. DCGAN utilizes a non-saturating objective function, which can be formulated in the form of the weighted sum of reverse Kullback-Leibler (KL) divergence and Jensen-Shannon (JS) divergence. This reverse KL loss is robust to gradient vanishing, however, easily falls into mode collapse [43]. Meanwhile, Fedus et. al [45] demonstrated experimentally that GP terms used by WGAN-GP and DRAGAN are effective for preventing mode collapse. Therefore, in order to investigate the effect of mode collapse on object localization, we compare DCGAN with WGAN-GP and DRAGAN.

**Data augmentation.** Data augmentation increases the amount of training data by adding processed images; for example, changing illuminations, adding noises, introducing occlusions, and etc. The augmented data is considered as the perturbation of original data, and is known to stabilize the network training. Recently, [33,34] introduced that this data augmentation improve localization performance for weakly-supervised object localization. Hence, we also expect that data augmentation can affect GAN-based unsupervised object localization. Specifically, we apply both photometric and spatial distortion used in GoogLeNet [7] to augment the data. Our experimental study shows how these techniques influence the learning process of GAN and the localization performance.

**Implementation details.** We decide hyperparameters and network architectures of selected GAN based on their papers [42,20,21]. While, for DRAGAN, we implement the non-saturating objective function as [45] recommended. The batch size of all GAN models is 128 and the training iteration is 200k. We choose CAM [12] among weakly-supervised approaches for the reference technique. Although the original implementation of CAM is built upon AlexNet and GoogLeNet, we replace the baseline CNN with pre-activation ResNet [46] to implement the CAM. Note that pre-activation ResNet is state-of-the-art CNN classification network. We choose the 34-layer architecture with batch size of 256. Training iteration is 100k. We also follow the original paper [46] to decide hyperparameters for implementing the ResNet-34. Specifically, we use a momentum optimizer, with momentum of 0.9. Learning rate is initially 0.1 decayed by a factor of 10 every 25k iterations. The weight decay is 1e-4.

## 5 Experimental results

In this section, we present our experimental results with analysis. First, we explain the dataset and evaluation metric used in the experiments. Then we report the experimental results of unsupervised object localization. We also perform co-localization experiments, a single category unsupervised object localization.

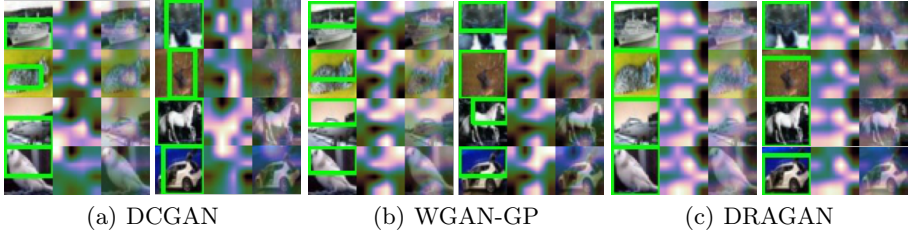


**Fig. 2.** Object localization results on CIFAR-10. In each figure, the left column is the input image, the middle, the extracted heatmap, while the right column is the result of overlapping heatmap and an input. We observe that heatmaps from DCGAN are focused according to locations of the main objects. On the other hand, the heatmaps of WGAN-GP and DRAGAN show the same part of the image regardless of the input image. This suggests that DCGAN may be vulnerable to mode collapse, but is advantageous for object localization.

Finally, we exam the relationship between mode collapse and localization performance through quantitative evaluation.

**Dataset.** Although ImageNet [47] is a popular benchmark dataset for recent object localization techniques, however, handling such high resolution dataset with GAN is another research problem. Hence, instead of ImageNet, we use low-resolution datasets, such as CIFAR-10 and Tiny ImageNet, which is simplified version of ImageNet. CIFAR-10 includes 10 categories, and with 5000 training images and 1000 test images per category. In Tiny ImageNet, there are 200 categories in total, and each category consists 500 training images, 50 validation images, and 50 test images.

**Evaluation metric.** We use the quantitative evaluation metric that is used in [33]. Specifically, we utilize localization accuracy with known ground-truth class (*GT-known Loc*). This metric considers to be correct only when the intersection of union (IoU) between estimated bounding box and the ground truth box is more than 50%. We also show qualitative evaluation by visualizing the bounding box and the heatmap. In the case of CIFAR-10 experiments, we only conduct qualitative evaluation, because there is no ground truth bounding box annotations. For Tiny ImageNet experiments, we analyze the results both qualitatively and quantitatively.

## 5.1 Fully-unsupervised object localization

**CIFAR-10.** We perform object localization using DCGAN, WGAN-GP, and DRAGAN with CIFAR-10 dataset. There are enough images to train GAN in this dataset, hence, we do not perform data augmentation in this case. Fig. 2 visualizes experimental results for each GAN; the first column shows the input image with the green bounding box, the second column illustrates heatmaps, and the third presents overlaps of the input with heatmaps. The results from DCGAN show that the bounding boxes reasonably capture the locations of the

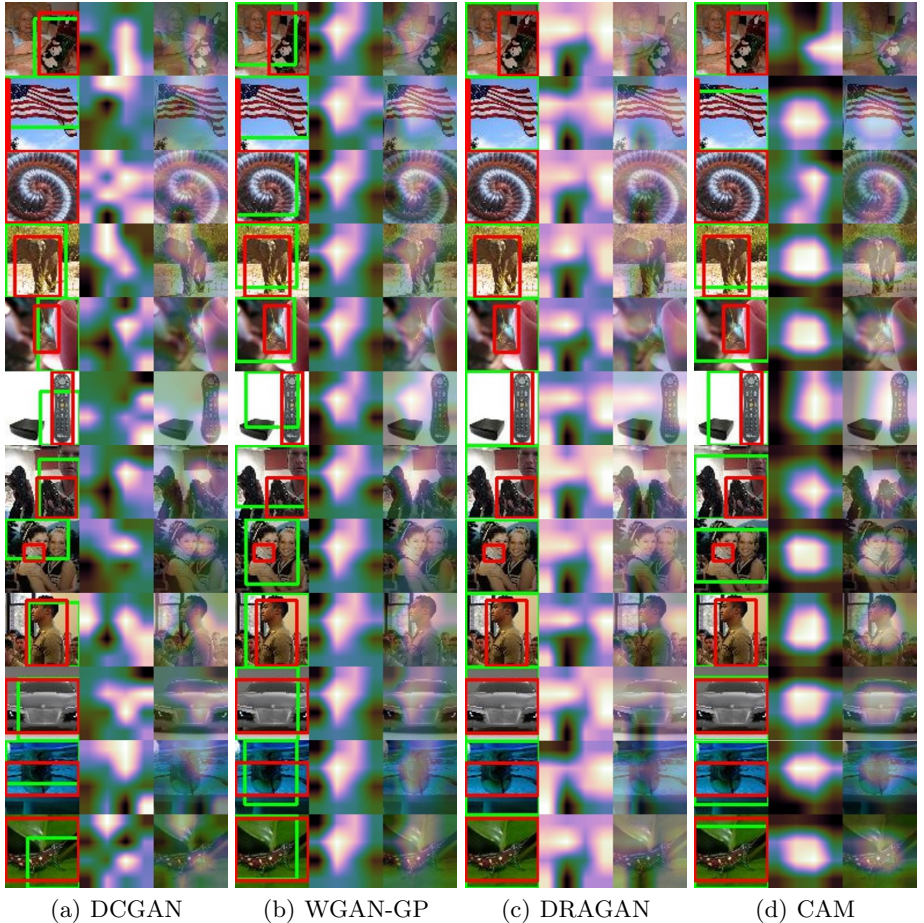


**Fig. 3.** Experimental results on Tiny ImageNet. The red bounding box is the ground truth, and the green box is our estimate. As in CIFAR-10 experiments, heatmaps from DCGAN is well positioned for main objects, while discriminators of WGAN-GP and DRAGAN look at same locations regardless of the input image. In rightmost, results of weakly-supervised approach show a clean heatmap and good localization performance.

dominant objects, also consistent with heatmaps, which significantly overlaps with the objects. In particular, in the case of ship and horse, we can observe that the heatmaps overlay even with the shapes of the target objects. However, the heatmaps from the WGAN-GP appear almost identical regardless of input images. The heatmaps from DRAGAN produce different shapes but their peaks are almost the same regardless of inputs.

We believe that this phenomenon is caused by characteristics of the objective function for each GAN, and the effect of the GP term. The Wasserstein distance

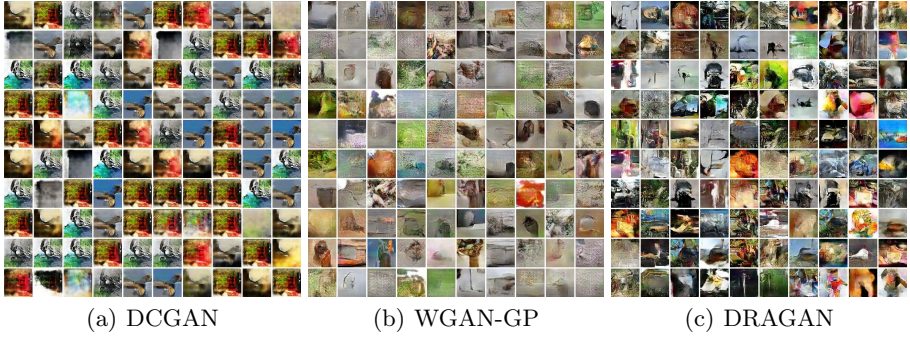


**Fig. 4.** Image samples generated by DCGAN, WGAN-GP, and DRAGAN when they produce localization results of Fig. 3. As we expected, DCGAN fall into a severe mode collapse while diverse images are generated by WGAN-GP and DRAGAN.

used in WGAN-GP is known to have a weak convergence property than non-saturating loss used in DCGAN. This property stabilizes GAN training, thus improving the diverse image generation [19]. In addition, the GP term used in WGAN-GP and DRAGAN leads GAN to learn various modes of the data distribution. Consequently, both WGAN-GP and DRAGAN are robust to mode collapse [45]. We believe that this is why the heatmaps from WGAN-GP and DRAGAN do not vary much upon the input images; the discriminator exams all objects, thus heatmaps do not focus on the dominant object.

**Tiny ImageNet.** We conduct both quantitative and qualitative evaluation using Tiny ImageNet dataset. Data augmentation is not applied for this experiment because the raw dataset is sufficiently large for training GAN. Fig. 3 compares both the bounding box and the heatmap from DCGAN, WGAN-GP, DRAGAN, and a weakly-supervised approach (CAM). Similar to CIFAR-10 experiments, heatmaps from DCGAN discriminator are quite effective in capturing the object position. On the other hand, heatmaps from discriminators of WGAN-GP and DRAGAN visualize almost identical area regardless of the input. To better understand the behavior of GANs, we observe the generated images from each GAN to analyze how the heatmap patterns affect image generation.

Fig. 4 shows examples of the generated images from DCGAN, WGAN-GP, and DRAGAN when they achieve localization results of Fig. 3. As expected, WGAN-GP and DRAGAN produce diverse images, which clearly exhibit that they learn various modes in dataset. Unlike them, the DCGAN generator repeatedly produce similar objects, a typical behavior of mode collapse. Based on such observations, we find that mode collapse and object localization have a positive correlation, thus WGAN-GP and DRAGAN are inappropriate to apply for object localization.

For the quantitative evaluation, we compare DCGAN and weakly-supervised methods by measuring GT-known Loc. The GT-known Loc of DCGAN is 41.4% while weakly-supervised approach (CAM) is 53.4%. Considering that our result

**Table 1.** The list of dataset for co-localization experiments.

Name	# train	# test	subcategory name
Artiodactyla	2500	250	bison, ox, bighorn, gazelle, arabian camel
Bottle	1000	100	pop bottle, beer bottle
Bird	1500	150	albatross, black stork, goose
Cat	2000	200	tabby, persian cat, egyptian cat, cougar
Dog	3000	300	standard poodle, yorkshire, golden retriever, labrador retriever, german shephered, chihuahua
Vehicle	4000	400	convertible, school bus, trolleybus, sports car, police van, moving van, limousine, beach wagon

is achieved under a fully unsupervised setting, we believe our performance is meaningful. One might argue that the GT-known Loc is biased because creating a large bounding box can increase the accuracy. It is a rational argument, hence, we have conducted both quantitative and qualitative assessment in this paper.

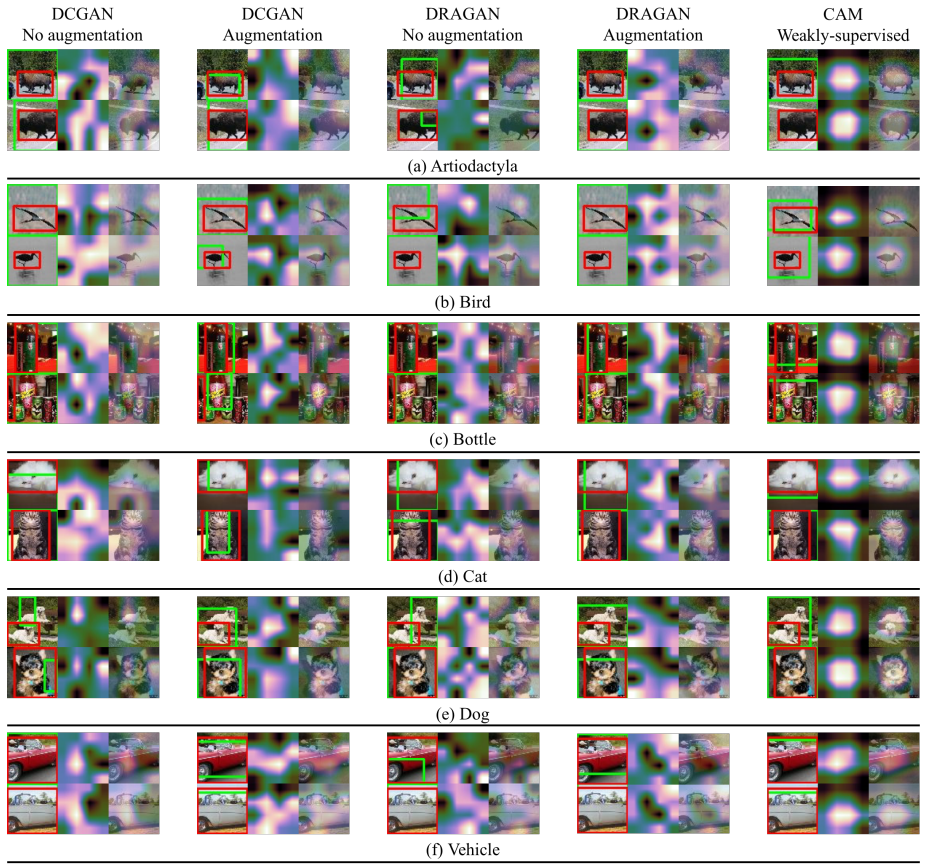
## 5.2 Co-localization

We combine similar categories in Tiny ImageNet and rearrange them for constructing six co-localization datasets. Table 1 shows the list of each co-localization dataset with the total number of images. Because the amount of images in each dataset is insufficient for training GAN, we apply data augmentation for these experiments.

We conduct object localization with six co-localization datasets using DC-GAN, WGAN-GP, and DRAGAN, respectively. Fig. 5 shows example results from six co-localization experiments. In these experiments, we observe that DC-GAN discriminator pays attentions to the location of a dominant object in the image as we intended. For WGAN-GP, the shapes of heatmaps from discriminator are similar regardless of the input as in previous experiments. Unlike previous experiments, DRAGAN discriminator also locates the dominant object when we do not apply data augmentation. However, with data augmentation, the shapes of heatmaps from DRAGAN discriminator are identical regardless of input, analogous to previous experiments.

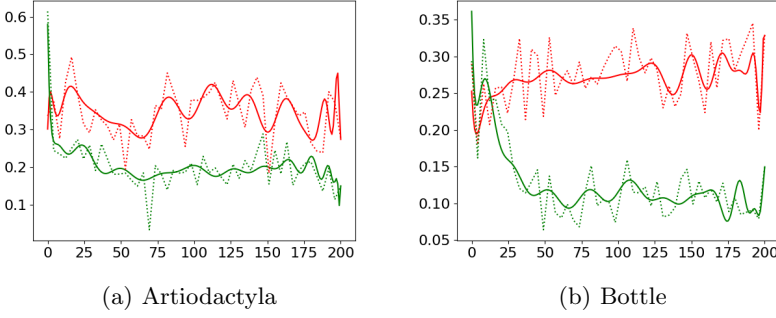
Data augmentation has the effect of increasing density of data distribution by perturbing the original data, and stabilizes the network training. Interestingly, in some cases, data augmentation has disadvantaged the object localization. In the case of DCGAN, diverse image generation is sacrificed to gain the visual quality of the generated image, while DRAGAN aims to improve both image quality and diversity. Therefore, data augmentation for DCGAN improves the image quality, which further enhances the process of learning the major modes of the data distribution. While, in DRAGAN, data augmentation enhances the process of learning various modes evenly, so that the discriminator exams all objects in the image.

Table 2 shows the quantitative evaluation results of DCGAN, DRAGAN, and weakly-supervised approach (CAM). Our co-localization results show slightly



**Fig. 5.** Experimental results of co-localization. Because WGAN-GP has a same problem as unsupervised experiments, we do not show the results of WGAN-GP in this figure. For DCGAN, data augmentation is helpful for localization performance. In the case of DRAGAN, the heatmap is extracted differently depending on the object without data augmentation, unlike the unsupervised experiments. However, when data augmentation is applied, the heatmaps from DRAGAN are almost identical regardless of input images, like the unsupervised experiments. The results from weakly-supervised approach show as good localization performance as previous experiments.

lower, but comparable, performance compared to the weakly-supervised approach. Interestingly, our approach shows superior performance in the Bottle dataset. This is because the dominant object in bottle dataset has a characteristic that it appears to have elongated shape in the image. The heatmaps from the proposed method appear to be in various shapes, while the heatmaps of the weakly-supervised method appear circular. These experimental results show that the GAN model better handles the elongated nature of the bottle than the



**Fig. 6.** Comparison between MS-SSIM and object localization accuracy. The red line indicates GT-known Loc and the green line indicates MS-SSIM. In addition, the horizontal axis denotes the number of training steps ( $\times 1000$ ), while the vertical axis shows the score of the each metric. The dotted line is the raw data and the solid line is the polynomial fitting curve of the raw data. We observe that the two graphs show similar trends.

**Table 2.** Quantitative evaluation results for co-localization experiments using GT-known Loc (%). Our results show slightly less performance compared to the weakly-supervised approach. We observe that data augmentation increases the localization performance of DCGAN. We also find that our proposed method perform better than weakly-supervised approach in the Bottle dataset. Interestingly, in the case of DRAGAN, the shapes of heatmaps are similar regardless of inputs when the data augmentation is applied. However, when augmentation is not applied, the discriminator searches only the dominant object in images. Therefore, we report only the results of DRAGAN without data augmentation in this table.

Dataset	DCGAN		DRAGAN	CAM
	w/o augment	w/ augment	w/o augment	weakly-supervised
Artiodactyla	41.4	43.0	50.0	53.4
Bird	49.3	52.3	49.3	57.0
Bottle	36.0	36.4	35.0	34.3
Cat	66.3	71.8	73.5	80.4
Dog	55.0	60.8	52.0	65.5
Vehicle	54.0	61.7	54.3	74.1

CNN classifier. Also, in the case of DCGAN, we observe that data augmentation increases object localization performance quantitatively.

We then verify more closely the relationship between localization performance and mode collapse in the co-localization setting. We use MS-SSIM [48] as a metric to quantitatively measure the degree of mode collapse in GAN. Higher the MS-SSIM means more severe mode collapse. Fig. 6 shows a graph comparing the performance of MS-SSIM and localization in Artiodactyla and Bottle experiments using DCGAN. We observe that the trends of MS-SSIM and object

localization performance are similar except for early stage of training. As a result, it seems to be closely related to the localization performance with MS-SSIM.

In addition, we are currently reporting the highest localization performance during training GAN without an explicit stop criteria. In the unsupervised approach, a stop criteria plays an important role because the localization performance significantly varies upon them. Based on the observation in Fig. 6, it is possible to utilize the MS-SSIM for developing the stop criteria. As a future work, we will study a stop criterion of GAN training for object localization, particularly using MS-SSIM.

## 6 Conclusions

In this paper, we propose the first end-to-end deep neural network model for unsupervised object localization. To this end, we train the GAN in an unsupervised manner, then visualize the region where GAN discriminator pays attention using CAM. Various experimental studies show that our approach has achieved meaningful performance for object localization in both qualitative and quantitative evaluations. When adopting the GAN model into the object localization problem, we found that there is a positive correlation between the mode collapse and object localization. Additionally, we observed that data augmentation can be effective in improving the localization performance of our DCGAN based model.

As a future work, because mode collapse is desirable for GAN-based object localization, the objective of our study may be opposite to regular GAN models. Therefore, we will design a novel GAN specialized for object localization. Furthermore, we find that the metric used in object localization (e.g., *GT-known Loc*) is not optimal for measuring localization performance. We will investigate a better metric for object localization.

## References

1. Ren, S., He, K., Girshick, R., Sun, J.: Faster R-CNN: Towards real-Time object detection with region proposal networks. *IEEE Transactions on Pattern Analysis and Machine Intelligence* **39**(6) (2017) 1137–1149
2. Redmon, J., Divvala, S., Girshick, R., Farhadi, A.: You only look once: Unified, real-Time object detection. In: *IEEE Conference on Computer Vision and Pattern Recognition*. (2016) 779–788
3. Liu, W., Anguelov, D., Erhan, D., Szegedy, C., Reed, S., Fu, C., Berg, A.: SSD: Single shot multibox detector. In: *European Conference on Computer Vision*. (2016) 21–37
4. Krizhevsky, A., Sutskever, I., Hinton, G.: Imagenet classification with deep convolutional neural networks. In: *Advances in Neural Information Processing Systems*. (2012) 1097–1105
5. Sermanet, P., Eigen, D., Zhang, X., Mathieu, M., Fergus, R., LeCun, Y.: OverFeat: Integrated recognition, localization and detection using convolutional networks. *arXiv:1312.6229* (2013)

6. Simonyan, K., Zisserman, A.: Very deep convolutional networks for large-scale image recognition. arXiv:1409.1556 (2014)
7. Szegedy, C., Liu, W., Jia, Y., Sermanet, P., Reed, S., Anguelov, D., Erhan, D., Vanhoucke, V., Rabinovich, A.: Going deeper with convolutions. In: IEEE Conference on Computer Vision and Pattern Recognition. (2015) 1–9
8. He, K., Zhang, X., Ren, S., Sun, J.: Deep residual learning for image recognition. In: IEEE Conference on Computer Vision and Pattern Recognition. (2016) 770–778
9. Girshick, R.: Fast R-CNN. In: IEEE International Conference on Computer Vision. (2015) 1440??–1448
10. Girshick, R., Donahue, J., Darrell, T., Malik, J.: Rich feature hierarchies for accurate object detection and semantic segmentation. In: IEEE Conference on Computer Vision and Pattern Recognition. (2014) 580–587
11. Redmon, J., Farhadi, A.: YOLO9000: Better, faster, stronger. In: IEEE Conference on Computer Vision and Pattern Recognition. (2017) 6517–6525
12. Zhou, B., Khosla, A., Lapedriza, A., Oliva, A., Torralba, A.: Learning deep features for discriminative localization. In: IEEE Conference on Computer Vision and Pattern Recognition. (2016) 2921–2929
13. Kim, G., Torralba, A.: Unsupervised detection of regions of interest using iterative link analysis. In: Advances in Neural Information Processing Systems. (2009) 961–969
14. Rubinstein, M., Joulin, A., Kopf, J., Liu, C.: Unsupervised joint object discovery and segmentation in internet images. In: IEEE Conference on Computer Vision and Pattern Recognition. (2013) 1939–1946
15. Tang, K., Joulin, A., Li, L., Fei-Fei, L.: Co-localization in real-world images. In: IEEE Conference on Computer Vision and Pattern Recognition. (2014) 1464–1471
16. Zhu, J., Wu, J., Xu, Y., Chang, E., Tu, Z.: Unsupervised object class discovery via saliency-guided multiple class learning. IEEE transactions on pattern analysis and machine intelligence **37**(4) (2015) 862–875
17. Cho, M., Kwak, S., Schmid, C., Ponce, J.: Unsupervised object discovery and localization in the wild: Part-based matching with bottom-up region proposals. In: IEEE Conference on Computer Vision and Pattern Recognition. (2015) 1201–1210
18. Goodfellow, I., Pouget-Abadie, J., Mirza, M., Xu, B., Warde-Farley, D., Ozair, S., Courville, A., Bengio, Y.: Generative adversarial nets. In: Advances in Neural Information Processing Systems. (2014) 2672–2680
19. Arjovsky, M., Chintala, S., Bottou, L.: Wasserstein GAN. arXiv:1701.07875 (2017)
20. Gulrajani, I., Ahmed, F., Arjovsky, M., Dumoulin, V., Courville, A.: Improved training of wasserstein GANs. In: Advances in Neural Information Processing Systems. (2017) 5769–5779
21. Kodali, N., Hays, J., Abernethy, J., Kira, Z.: On convergence and stability of GANs. arXiv:1705.07215 (2017)
22. Bilen, H., Pedersoli, M., Tuytelaars, T.: Weakly supervised object detection with posterior regularization. In: British Machine Vision Conference. (2014) 1–12
23. Song, H., Girshick, R., Jegelka, S., Mairal, J., Harchaoui, Z., Darrell, T.: On learning to localize objects with minimal supervision. arXiv:1403.1024 (2014)
24. Cinbis, R., Verbeek, J., Schmid, C.: Multi-fold MIL training for weakly supervised object localization. In: IEEE Conference on Computer Vision and Pattern Recognition. (2014) 2409–2416
25. Song, H., Lee, Y., Jegelka, S., Darrell, T.: Weakly-supervised discovery of visual pattern configurations. In: Advances in Neural Information Processing Systems. (2014) 1637–1645

26. Li, D., Huang, J., Li, Y., Wang, S., Yang, M.: Weakly supervised object localization with progressive domain adaptation. In: IEEE Conference on Computer Vision and Pattern Recognition. (2016) 3512–3520
27. Cinbis, R., Verbeek, J., Schmid, C.: Weakly supervised object localization with multi-fold multiple instance learning. *IEEE Transactions on Pattern Analysis and Machine Intelligence* **39**(1) (2017) 189–203
28. Simonyan, K., Vedaldi, A., Zisserman, A.: Deep inside convolutional networks: Visualising image classification models and saliency maps. arXiv:1312.6034 (2013)
29. Oquab, M., Bottou, L., Laptev, I., Sivic, J.: Is object localization for free? - Weakly-supervised learning with convolutional neural networks. In: IEEE Conference on Computer Vision and Pattern Recognition. (2015) 685–694
30. Bilen, H., Vedaldi, A.: Weakly supervised deep detection networks. In: IEEE Conference on Computer Vision and Pattern Recognition. (2016) 2846–2854
31. Kantorov, V., Oquab, M., Cho, M., Laptev, I.: ContextLocNet: Context-Aware deep network models for weakly supervised localization. In: European Conference on Computer Vision. (2016) 350–365
32. Kim, D., Cho, D., Yoo, D., Kweon, I.: Two-Phase learning for weakly supervised object localization. In: IEEE International Conference on Computer Vision. (2017) 3554–3563
33. Singh, K., Lee, Y.: Hide-and-Seek: Forcing a network to be meticulous for weakly-supervised object and action localization. In: IEEE International Conference on Computer Vision. (2017) 3544–3553
34. Choe, J., Park, J., Shim, H.: Improved techniques for weakly-supervised object localization. arXiv:1802.07888 (2018)
35. Joulin, A., Bach, F., Ponce, J.: Discriminative clustering for image co-segmentation. In: IEEE Conference on Computer Vision and Pattern Recognition. (2010) 1943–1950
36. Wei, X., Zhang, C., Li, Y., Xie, C., Wu, J., Shen, C., Zhou, Z.: Deep descriptor transforming for image co-localization. In: International Joint Conference on Artificial Intelligence. (2017) 3048–3054
37. Wei, X., Zhang, C., Wu, J., Shen, C., Zhou, Z.: Unsupervised object discovery and co-localization by deep descriptor transforming. arXiv:1707.06397 (2017)
38. Niu, Z., Hua, G., Wang, L., Gao, X.: Knowledge-based topic model for unsupervised object discovery and localization. *IEEE Transactions on Image Processing* **27**(1) (2018) 50–63
39. Sivic, J., Russell, B., Efros, A., Zisserman, A., Freeman, W.: Discovering objects and their location in images. In: IEEE Conference on Computer Vision and Pattern Recognition. Volume 1. (2005) 370–377
40. Andrzejewski, D., Zhu, X., Craven, M.: Incorporating domain knowledge into topic modeling via dirichlet forest priors. In: International Conference on Machine Learning, ACM (2009) 25–32
41. Chang, J., Gerrish, S., Wang, C., Boyd-Graber, J., Blei, D.: Reading tea leaves: How humans interpret topic models. In: Advances in Neural Information Processing Systems. (2009) 288–296
42. Radford, A., Metz, L., Chintala, S.: Unsupervised representation learning with deep convolutional generative adversarial networks. arXiv:1511.06434 (2015)
43. Arjovsky, M., Bottou, L.: Towards principled methods for training generative adversarial networks. arXiv:1701.04862 (2017)
44. Cesa-Bianchi, N., Lugosi, G.: Prediction, learning, and games. Cambridge university press (2006)

45. Fedus, W., Rosca, M., Lakshminarayanan, B., Dai, A.M., Mohamed, S., Goodfellow, I.: Many paths to equilibrium: GANs do not need to decrease a divergence at every step. arXiv:1710.08446 (2017)
46. He, K., Zhang, X., Ren, S., Sun, J.: Identity mappings in deep residual networks. In: European Conference on Computer Vision. (2016) 630–645
47. Russakovsky, O., Deng, J., Su, H., Krause, J., Satheesh, S., Ma, S., Huang, Z., Karpathy, A., Khosla, A., Bernstein, M., Berg, A., Fei-Fei, L.: ImageNet large scale visual recognition challenge. International Journal of Computer Vision **115**(3) (2015) 211–252
48. Odena, A., Olah, C., Shlens, J.: Conditional image synthesis with auxiliary classifier GANs. arXiv:1610.09585 (2016)